Accepted: 23 March 2018

DOI: 10.1111/epi.14083

FULL-LENGTH ORIGINAL RESEARCH PAPER

Epilepsia®

Longitudinal positron emission tomography imaging of glial cell activation in a mouse model of mesial temporal lobe epilepsy: Toward identification of optimal treatment windows

Duc-Loc Nguyen[1] | Catriona Wimberley[1] | Charles Truillet[1] | Benoit Jego[1] | Fabien Caillé[1] | Géraldine Pottier[1] | Raphaël Boisgard[1] | Irène Buvat[1] | Viviane Bouilleret[1,2]

[1]In Vivo Molecular Imaging Laboratory (IMIV), French National Institute of Health and Medical Research (INSERM), French Alternative Energies and Atomic Energy Commission (CEA), French National Center for Scientific Research (CNRS), Paris Saclay University, Frédéric Joliot Hospital service, Orsay, France

[2]Neurophysiology and Epilepsy Unit, Bicêtre Hospital, Public Hospitals of Paris (AP-HP), France

Correspondence
Charles Truillet, In Vivo Molecular Imaging Laboratory (IMIV), French National Institute of Health and Medical Research (INSERM), French Alternative Energies and Atomic Energy Commission (CEA), French National Center for Scientific Research (CNRS), Paris Saclay University, Frédéric Joliot Hospital service, Orsay, France.
Email: charles.truillet@cea.fr

Summary

Objective: Mesiotemporal lobe epilepsy is the most common type of drug-resistant partial epilepsy, with a specific history that often begins with status epilepticus due to various neurological insults followed by a silent period. During this period, before the first seizure occurs, a specific lesion develops, described as unilateral hippocampal sclerosis (HS). It is still challenging to determine which drugs, administered at which time point, will be most effective during the formation of this epileptic process. Neuroinflammation plays an important role in pathophysiological mechanisms in epilepsy, and therefore brain inflammation biomarkers such as translocator protein 18 kDa (TSPO) can be potent epilepsy biomarkers. TSPO is associated with reactive astrocytes and microglia. A unilateral intrahippocampal kainate injection mouse model can reproduce the defining features of human temporal lobe epilepsy with unilateral HS and the pattern of chronic pharmacoresistant temporal seizures. We hypothesized that longitudinal imaging using TSPO positron emission tomography (PET) with ^{18}F-DPA-714 could identify optimal treatment windows in a mouse model during the formation of HS.

Methods: The model was induced into the right dorsal hippocampus of male C57/Bl6 mice. Micro-PET/computed tomographic scanning was performed before model induction and along the development of the HS at 7 days, 14 days, 1 month, and 6 months. In vitro autoradiography and immunohistofluorescence were performed on additional mice at each time point.

Results: TSPO PET uptake reached peak at 7 days and mostly related to microglial activation, whereas after 14 days, reactive astrocytes were shown to be the main cells expressing TSPO, reflected by a continuing increased PET uptake.

Significance: TSPO-targeted PET is a highly potent longitudinal biomarker of epilepsy and could be of interest to determine the therapeutic windows in epilepsy and to monitor response to treatment.

KEYWORDS
glial cells activation, neuroinflammation, TSPO PET, unilateral intrahippocampal kainate injection mouse model

1 | INTRODUCTION

The current spectrum of antiepileptic drugs (AEDs) consists of symptomatic treatments that are effective in the majority of patients with epilepsy. However, around 30% of patients remain pharmacoresistant, reflecting the complex and multifaceted mechanisms underlying epilepsy.[1] Although progress has been made in the development of the newer generation of AEDs, no treatment can currently modify epileptogenesis or prevent, stop, or cure epilepsy. Therefore, there is an urgent need for new therapies that would target altered pathways complementary to those currently treated by AEDs.

Recent crucial findings regarding neuroinflammation have drawn attention to pathophysiological mechanisms that might play a significant role in epilepsy.[2] Therefore, in subjects with pharmacoresistant epilepsy, neuroinflammation can be explored as a biomarker of seizure focus[3,4] and frequency.[5–7] From this, neuroinflammation could also be a target for the development and monitoring of novel therapies.[8] Translocator protein 18 kDa (TSPO) expression is associated with neuroinflammatory processes involving reactive astrocytes and microglia.[9] TSPO is expressed at low levels in healthy brain but is markedly increased at sites of brain injury and inflammation, making it of great interest as a biomarker for the study of diseases that include a component of neuroinflammation.[10]

TSPO positron emission tomography (PET) is currently a reference tool for monitoring neuroinflammation involved in many brain diseases such as Alzheimer disease,[11] stroke,[12] traumatic brain injury,[13] multiple sclerosis,[14] amyotrophic lateral sclerosis,[15] and brain tumors.[16] There have also been studies in humans reporting increased TSPO binding in different types of epilepsy such as Rasmussen encephalitis,[17] focal cortical dysplasia,[4] and mesial temporal lobe epilepsy (MTLE).[3] TSPO expression in the central nervous system is commonly associated with microglial activation. However, TSPO has been proven to be expressed in different cell types such as astrocytes and endothelial cells and the similarities and differences in TSPO expression mechanisms between humans and rodents has to be well recognized and handled.[18] The rodent model should be chosen in association with human data and as a function of the disease step to be investigated.

There are a number of pharmacoresistant models of epilepsy in rodents, but the model with the unilateral injection of kainate in mice has been shown to be the closest to the human pathology.[19–21] The similarities include a unilateral lesion that is limited to the hippocampus, with a pattern of classical unilateral hippocampal sclerosis (HS) and a persistent lifetime of spontaneous recurrent seizures. In rat models of epilepsy induced by kainic acid (KA) or by pilocarpine,[7,22] the lesions are often not confined to the hippocampus, as in human MTLE. TSPO PET imaging of these rat models has shown a transient peak uptake within the limbic system, reaching its maximum at 7 days after status epilepticus (SE) but declining toward baseline at 14-16 weeks post-SE. Only one very recent longitudinal study in KA mice has shown persistent TSPO expression up to 3 months.[23]

Our objective was to monitor the evolution of TSPO PET signal using ^{18}F-DPA-714 to determine which glial cells were involved during the formation of the HS using immunofluorescence in a longitudinal study of this mouse model of epilepsy.

Key Points

- Longitudinal TSPO PET imaging with ^{18}F-DPA-714 can follow the progression of MTLE in small brain structures of the mouse, such as the hippocampus
- The different components of glial activation relative to the longitudinal PET signal during the formation of HS were determined using immunofluorescence
- The persistently high TSPO signal in the established HS shows chronic activation of astrocytes, which suggests a new possible treatment window in drug-resistant epilepsy

2 | MATERIALS AND METHODS

2.1 | Animal models

All experiments were performed under an animal use and care protocol approved by the Animal Ethics Committee and were conducted in accordance with the European Union regulations on animal research.

Experiments were performed on adult C57Bl/6 male mice (4 months old; Charles River, Saint-Germain-Nuelles, France) housed in individual cages with food and water ad libitum and kept in a 12-hour light-dark controlled cycle. Mice were anesthetized with isoflurane and placed in a stereotaxic frame. Injections were made using a 30-gauge removable needle (Hamilton Company, Reno, NV, USA) connected to a 10-μL microsyringe. KA (Sigma-Aldrich, St. Louis, MO, USA) dissolved in 0.9% saline (50 nL, 0.2 μg) was injected over 1 minute using an automatic syringe pump into the right dorsal hippocampus (anteroposterior, −1.8 mm; mediolateral, −1.6 mm; dorsoventral, −1.8 mm) with bregma as reference.[21] After injection, the needle was maintained in situ for an additional 1 minute to limit reflux along the injection track. Sham mice were also prepared by injecting 50 nL of 0.9% saline at the same location using the same procedure.

The KA model was induced in 20 mice for PET imaging and in vitro autoradiography and immunofluorescence. Upon recovery from anesthesia, all of them showed at least 1 characteristic of SE such as immobility, rotations, or mild clonic movements of the forelimbs that lasted for up to 48 hours as previously described.[21] No treatment was administered after induction of SE. Three mice died within 1-2 days after surgery. Fifteen sham mice were prepared, and none died after surgery.

2.2 | Experimental design

For PET imaging, epileptic mice underwent ^{18}F-DPA-714 scans before model induction (baseline, n = 9) and at 7 and 14 days (n = 6), 1 month (n = 8), and 6 months (n = 8) after the model induction (Figure S1). Sham mice were scanned with the exact same procedure to obtain scans at baseline (n = 8), 7 days (n = 5), 14 days (n = 4), 1 month (n = 8), and 6 months (n = 6). Repeated scans of the same animals were performed whenever possible. Not all animals could be scanned at all time points, because the number of scans per day was limited due to the decay of specific radioactivity and/or the failure of injection.

All mice from the longitudinal PET studies were euthanized at 6 months to confirm HS. Three further cohorts of baseline, KA, and sham mice were prepared specifically for in vitro autoradiography and immunohistochemistry, and 3 mice from each cohort were euthanized at each time point corresponding to the time points of the PET scans.

2.3 | PET imaging procedure

^{18}F-DPA-714 was synthesized as previously described.[24] Mice were anesthetized with isoflurane (3.5% for induction, 1.5%-2% for maintenance of anesthesia). Static PET scans of 60 minutes were acquired immediately after a tail vein injection of 2.59-15.45 MBq of ^{18}F-DPA-714 (injected mass = 0.05-0.25 ng; specific activity = 34.52-407 GBq/μmol, in a volume of 100 μL) using a micro-PET/computed tomographic (CT) device (Inveon PET-CT; Siemens Medical Solutions, Erlangen, Germany). After the static PET, a CT scan was performed for attenuation correction and also for registering PET/CT images to a magnetic resonance imaging (MRI) template. Images were reconstructed using a 2-dimensional ordered subset expectation maximization (OSEM) iterative algorithm, without any postfiltering.

2.4 | PET image analysis

PET images were automatically coregistered to the CT scan. Skull CT contours were manually coregistered to the Mirrione MRI template atlas.[25] The combination of 2 transformations was used to overlay the PET and MRI images. All image processing was performed using Pmod 3.6 software (PMOD Technologies, Zurich, Switzerland). The regions of interest including right and left hippocampus and other extrahippocampal regions (cortex, thalamus, amygdala, and cerebellum) were identified per the Mirrione atlas. The ^{18}F-DPA-714 uptake of each region was calculated as percentage injected dose per cubic centimeter of tissue (%ID/cc) over the 60-minute scan. The uptake of each region was then normalized to the uptake in the cerebellum, which was not significantly different at any time point compared to baseline level (Figure 1). The choice of this region for normalization is also supported by other publications.[14]

2.5 | In vitro autoradiography and immunohistofluorescence

To validate and interpret in vivo measurements, at each time point, the animals were maintained under strong anesthesia (4% isoflurane) and the mouse brain was washed via transcardiac perfusion with saline 0.9% through the left ventricle. Brains were harvested and snap-frozen in 2-methylbutane and stored at −80°C. Serial coronal sections (10-μm thickness) were collected and mounted on coated glass slides (Superfrost Ultra Plus; Thermo Fisher Scientific, Waltham, MA, USA) using a cryostat (CM3050; Leica, Wetzlar, Germany) and stored at −80°C until autoradiography or immunohistochemistry was performed. For each mouse brain, serial coronal sections were collected at −1.34, −1.58, −1.82 mm (dorsal hippocampus) and −2.3, −2.70, −3.28 mm (ventral hippocampus) from bregma.[26] The anatomy of brain sections was confirmed by hematoxylin and eosin staining (Figure S3).

2.5.1 | ^{18}F-DPA-714 in vitro autoradiography

The brain coronal sections were incubated in 37 MBq of ^{18}F-DPA-714 for 20 minutes at 4°C. They were then washed twice for 2 minutes in 50 mmol/L tris-HCl (pH = 7.4) buffer at 4°C. After a quick dip in ice-cold distilled water, the slides were dried. Autoradiography was then obtained by exposing the slides, placed in a cassette at room temperature, to a high-performance phosphor storage screen for 24 hours. The screens were read using a Storm scanner.

For the semiquantification of the autoradiography, we analyzed 6 sections per mouse. For each section, regions were manually drawn within the right and left hippocampus, thalamus, cortex, and right and left amygdala. For each region i, the mean signal intensity value R_i over the sections in which the region was present was calculated. In addition, in each mouse j, the mean cerebellum signal intensity ($Cereb_j$) was calculated over 5 additional sections in which the cerebellum was present. For each mouse j, the signal in each target region was normalized by dividing the

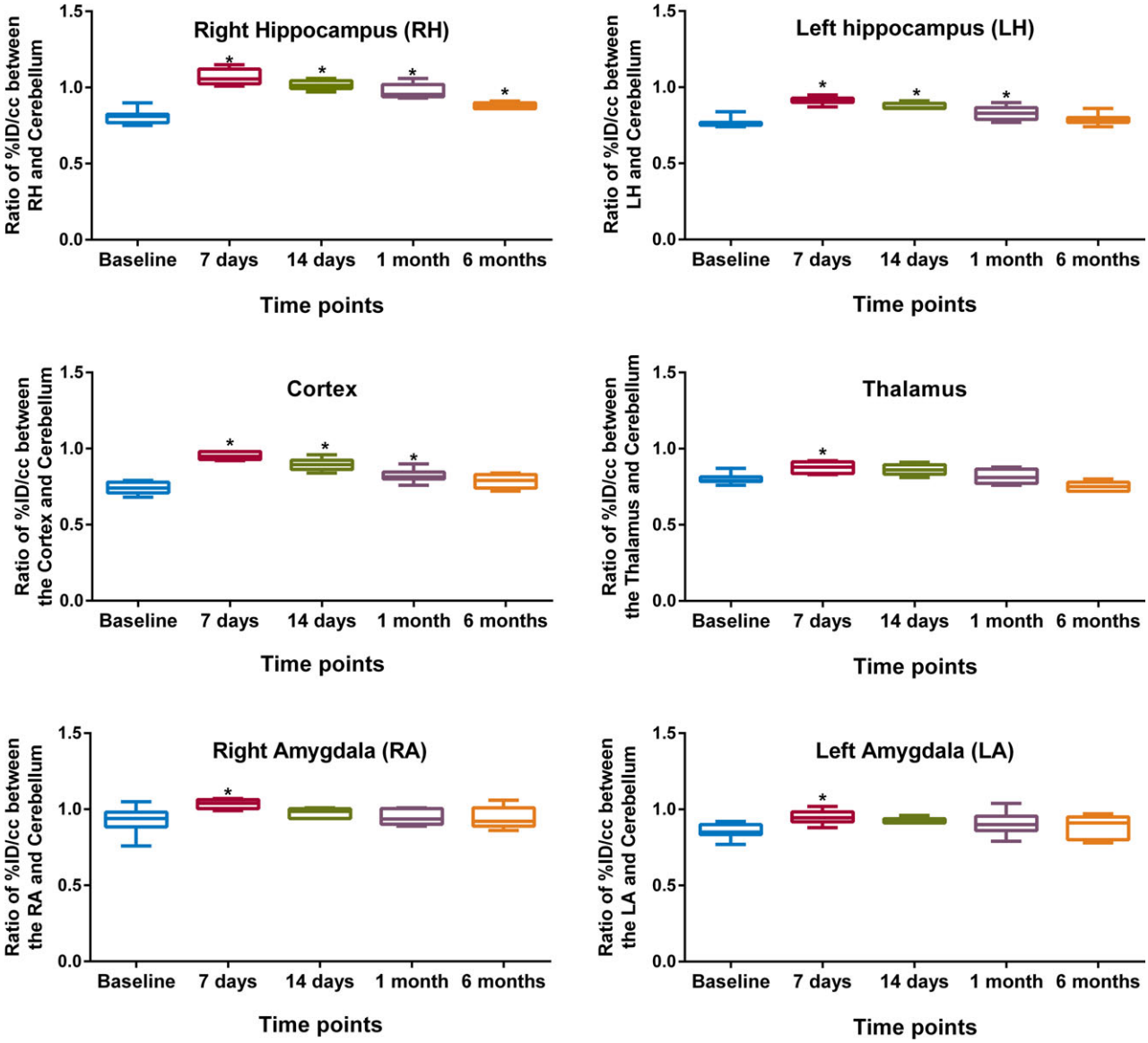

FIGURE 1 Percentage injected dose per cubic centimeter of tissue (%ID/cc) ratio of 18F-DPA-714 uptake in the hippocampi and other extrahippocampal regions compared to 18F-DPA-714 uptake in cerebellum at the different imaging times in the kainic acid (KA)-injected group. The uptake of 18F-DPA-714 in the KA group displays significant differences between the different time points for the right hippocampus (*$P < .05$) at every time point (n = 6 mice for KA group)

average value R_i measured in that region i by the mouse-specific average cerebellum signal intensity Cereb: R_i/Cereb$_j$. The autoradiography image analysis was conducted using ImageJ (National Institutes of Health, Bethesda, MD, USA).

2.6 | Immunofluorescence

2.6.1 | Triple staining TSPO/CD11b/glial fibrillary acidic protein

Cryostat brain sections were fixed with 10% paraformaldehyde, blocked with 5% bovine serum albumin and 0.5% Tween, and then incubated for 1 hour at temperature room with a rabbit monoclonal primary antibody against TSPO (anti-PBR antibody [EPR5384], 1:500; Abcam, Cambridge, MA, USA), a rat monoclonal primary antibody against CD11b (Abcam, 1:500), and a chicken monoclonal primary antibody against glial fibrillary acidic protein (GFAP; Abcam, 1:500). Then the sections were rinsed twice and incubated for 30 minutes at room temperature with a secondary antirabbit antibody (Alexa Fluor 488, 1:1000), a secondary antirat antibody (Alexa Fluor 564, 1:1000), and a secondary antichicken antibody (Alexa Fluor 647, 1:1000). Sections were counterstained with 4,6-diamidino-2-phenylindole (DAPI) to visualize the cell nuclei.

A mosaic acquisition with a magnification of 20× was performed, entirely covering the brain section using an Axio Observer Z1 microscope (Carl Zeiss, Oberkochen,

Germany). The fusion of mosaic images were generated by AxioVision 4.6 (Carl Zeiss). A sequential acquisition of separate wavelength channels was used to avoid fluorescence crosstalk. Exposure times were set so that pixel brightness was never saturated and kept constant during the entire image acquisition and between different experiments.

To visualize the TSPO and glial distribution, a constant threshold method (moments dark)[27] was applied to the mosaic images for each channel using ImageJ. To visualize the colocalization, the staining was adjusted on images captured at the hilus so that an optimal representation of TSPO, microglia, and astrocyte was achieved.

2.6.2 | Double staining TSPO/CD31

To determine whether there was a colocalization between endothelial cells and TSPO, we also performed a double staining TSPO/CD31 with a rat monoclonal primary antibody against CD31 (1:500; BD Biosciences, Franklin Lakes, NJ, USA) and a secondary antirat antibody (Alexa Fluor 564, 1:1000). Sections were counterstained with DAPI to visualize the cell nuclei.

2.7 | Statistical analysis

All data were analyzed using nonparametric tests, and results were presented as median (25% percentile-75% percentile). For in vivo PET images, Wilcoxon matched pairs signed-rank tests were performed to compare the signal between each time point and the baseline of the same animal to reduce the intersubject variability. For longitudinal analysis at all time points, Pearson coefficient was used only on the same animals. Animals with missing time points were not included in the statistical test. For autoradiography, the baseline mice and the sham mice of each time point were grouped to create a control group. Mann-Whitney *U* test was performed to compare the KA group at each time point with the control group. Analyses were performed using Prism 6 software (GraphPad Software, La Jolla, CA, USA). Values of $P < .05$ were interpreted as statistically significant.

3 | RESULTS

3.1 | Evolution of ^{18}F-DPA-714 uptake in longitudinal PET study

In the epilepsy mice (KA group), compared to the baseline level (Figure 2A,B), the signal reached a peak at 7 days, predominantly in the injected hippocampus (2.10%ID/cc [1.84-2.28], $P = .03$). The signal in the contralateral hippocampus decreased gradually and returned to baseline level at 1 month. The signal in the injected hippocampus also decreased but always remained significantly higher than baseline even 6 months after injection of KA (1.85% ID/cc [1.55-1.98], $P = .02$). To evaluate the surgical effect, we compared the KA population and the sham population (saline injection). At any time point after injection, the TSPO PET signal of KA-injected hippocampus was always significantly higher compared to saline-injected hippocampus, even 6 months after injection (Figure 2C). In the sham mice, for all time points, there was no significant difference in the PET signal observed in the hippocampus regions compared to the signal in the same region at baseline (Figure S2B).

In the KA mice, at 7 days, a high uptake was observed across all brain regions (hippocampus, cortex, thalamus, and amygdala) in both hemispheres (Figure 2B), except for the cerebellum (Figure S2A). At 14 days, the uptake of all regions outside the hippocampus returned to baseline, except for the cortex. At 6 months, the cortex signal was no longer significantly different from the baseline level.

3.2 | In vitro autoradiography and TSPO immunofluorescence

The visual analysis of the brain sections of the baseline mice showed an intense and localized signal in the lateral ventricles and third ventricle only (Figure 3A,C). In the sham mice, we observed a localized signal along the needle track at 7 and 14 days after surgery, and this signal was no longer observed after 1 month (Figure 3A). In the KA mice, in vitro ^{18}F-DPA-714 autoradiography confirmed the high TSPO signal in the injected hippocampus at all time points, even up to 6 months (Figure 3C). The high TSPO signal was also observed in the contralateral hippocampus at lower magnitude but was no longer observed after 1 month. In the images in Figure 3B,D, TSPO immunofluorescence images at the different time points show excellent spatial agreement with autoradiographic images of the sham and KA groups. Outside the hippocampus, a high localized signal was observed in the right cortex between 7 and 14 days (Figure 3C), predominantly at the injected site. There was also a high localized signal in basolateral amygdala nucleus, just beneath the lateral ventricle, and in lateral nuclei of the right thalamus in some KA mice at some time points between 7 days and 1 month involving preferentially the ipsilateral thalamus, as summarized in Figure S4.

For the in vitro autoradiography results (Figure 4A,B), the signal also reached a peak at 7 days in the hippocampi, predominantly in the right hippocampus ($P = .023$). The signal in the right hippocampus decreased at 6 months but remained significantly higher than in the control ($P = .047$). The signal in the left hippocampus returned to baseline level at 1 month. Figure 4C,D also showed a good

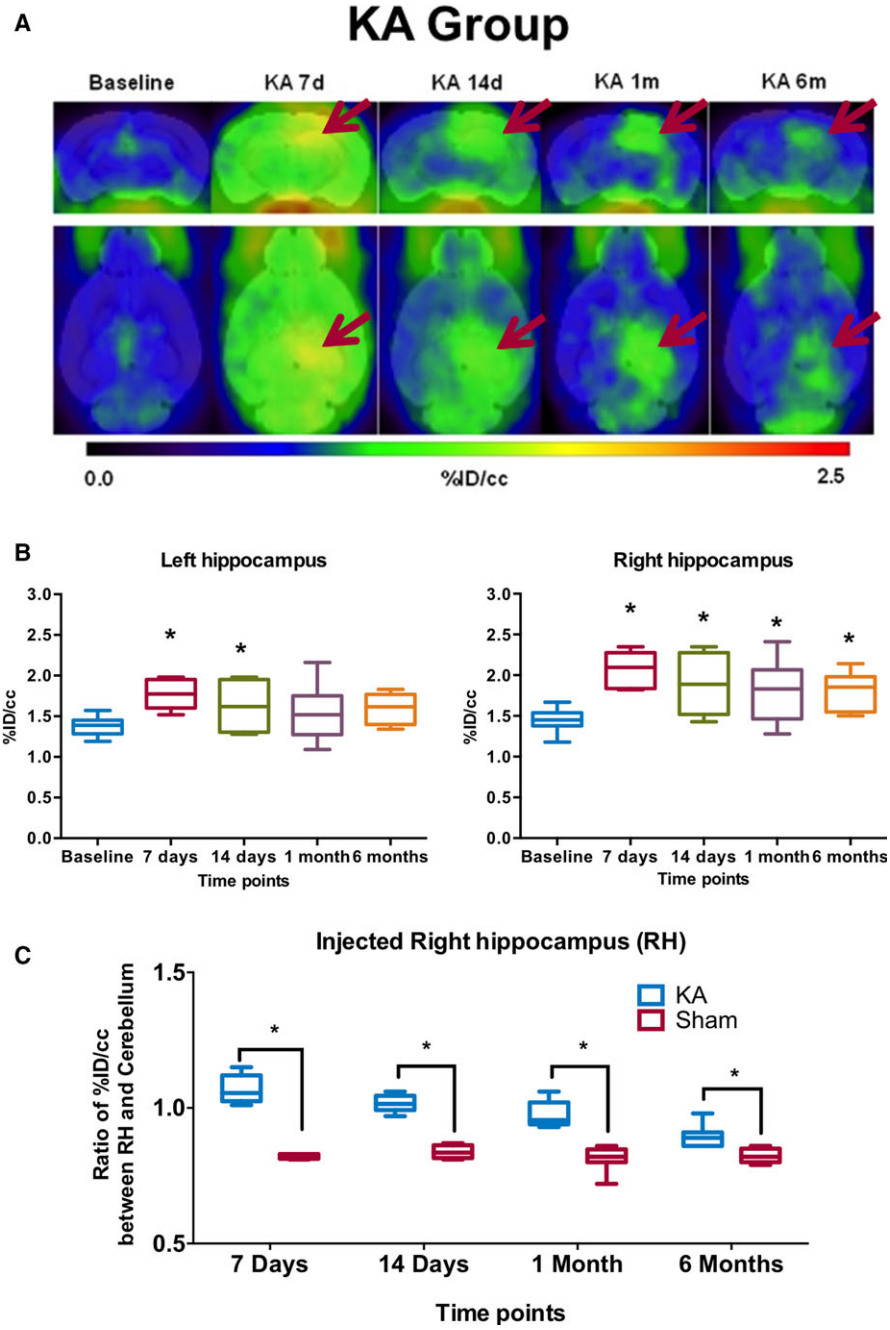

FIGURE 2 Longitudinal translocator protein (TSPO) positron emission tomography (PET) imaging in the kainic acid (KA)-injected group. A, Representative coronal and transaxial brain images of 18F-DPA-714 (percentage injected dose per cubic centimeter of tissue [%ID/cc]) from the same subject at 5 different time points (baseline, 7 days, 14 days, 1 month, and 6 months; n = 6 mice for KA group and n = 4 mice for sham group). B, Uptake of 18F-DPA-714 in %ID/cc over the whole 60-minute scan in the left (no lesion) and right hippocampus (KA injection) at each time point. The uptake of 18F-DPA-714 in the right hippocampus of the KA group is significantly different from baseline at all time points, unlike in the left hippocampus. C, PET signal ratio between the right hippocampus and cerebellum in the KA and sham groups. The TSPO signal at any time point after KA injection is significantly greater than TSPO signal after saline injection in the injected hippocampus (*$P < .05$)

agreement between autoradiography and PET signal. The high signal in the cortex, thalamus, and amygdala was observed only at 7 days. No significant difference of PET signal was observed in any other brain region even 7 days after KA injection (Figure S5). The agreement between autoradiography and PET signal was also observed in these extrahippocampal regions, but at a lower level.

3.3 | Evolution of the glial activation pattern during the formation of HS

DAPI images (Figure 5, blue staining) confirmed localized HS at 6 months after KA injection in the injected hippocampus with a neuronal cell loss in the CA1 and CA3 (a-c) of pyramidal layers and granular cell dispersion at the dentate gyrus. No structural changes were detected in the contralateral hippocampus.

3.3.1 | Microglia

At baseline, microglia presented with low CD11b signal, thin ramifications, and small soma (Figures 5A, 6). At 7 days after injection, intense CD11b-positive cells with large body and thick process were observed bilaterally, predominantly in the hilus and the CA3 (a-c) cell layer of the ipsilateral hippocampus. In the contralateral region,

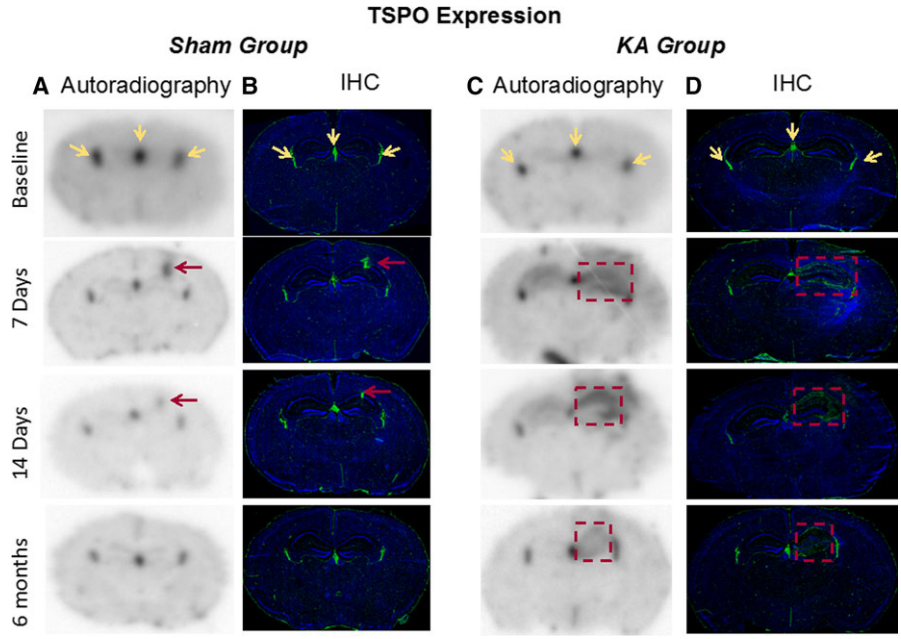

FIGURE 3 In vitro distribution of translocator protein (TSPO) expression in coronal slices of a baseline mouse brain (without injection) and of a mouse brain at different points of time after saline (sham) and kainic acid (KA) injection (7 days, 14 days, and 6 months). A, C, The region of interest (injected hippocampus) is shown by a red square; yellow arrows show the lateral and third ventricles, whereas the red arrows point to the needle track. B, D, Representative autoradiographic images of the brain coronal slice after incubation of the specific TSPO tracer ^{18}F-DPA-714 for the sham and KA groups, respectively. Immunohistochemical (IHC) distribution of mouse TSPO monoclonal antibody is shown in coronal slices of a mouse brain for the sham and KA groups. An excellent agreement between the TSPO detected via monoclonal antibody and the radioactive DPA is observed with a high accumulation of the 2 biomarkers at 7 days and 14 days

microglial activation was not observed within the pyramidal cell layer but distributed only in the strata oriens and lucidum (Figure S6). At 14 days, CD11b signal decreased clearly in both the contralateral hippocampus and the hilus of the injected hippocampus. The signal remained increased within the ipsilateral CA1 and CA3c layers and the corresponding strata oriens and lucidum. CD11b signal continued to decrease at 1 month and remained very low at 6 months when HS was fully established. Only CD11b-positive cells with a round amoeboid shape were visualized in the neuron-depleted pyramidal zone.

3.3.2 | Astrocytes

At baseline, similar to microglia, astrocytes showed a low GFAP signal with small body and thin branches (Figures 5C, 6). At 7 days, GFAP signal increased bilaterally with more and better-visualized branches. At 14 days, GFAP signal decreased in contralateral hippocampus but never returned to baseline level, even 6 months after injection (Figure S6). Conversely, GFAP cells were denser in the ipsilateral hippocampus and more pronounced with time, especially at 6 months, showing severely reactive and scar-forming astrocytes in the neuronal death zone but also within the dispersed granular layer.

3.4 | Time course of TSPO expression by different cells along the disease process

At baseline level, the TSPO signal was low, and it principally came from endothelial cells. In Figure S8, the baseline brain slices were stained using the endothelial biomarker CD31 which revealed the colocalization of the endothelial cells and TSPO. CD11b and GFAP staining showed low or absent colocalization with TSPO (Figure 6). The influence of the endothelial TSPO contribution over time is shown in Figure S7, and a magnification of some TSPO colocalizing with endothelial cells at 6 months is displayed in Figure S9.

Spatial TSPO distribution (Figure 5B) correlated well with the CD11b signal at 7 and 14 days and with GFAP signal at 6 months after KA injection.

At 7 days after KA injection, intense TSPO signal was observed in the whole ipsilateral hippocampus, predominantly in the hilus, which principally came from microglial activation (Figure 6). From 14 days to 1 month, TSPO microglia decreased clearly in the hilus but persisted in the CA1 and CA3c pyramidal layer. An increased TSPO signal was also observed in some astrocytes but to a lower extent than that seen within the microglia cells.

At 6 months after KA injection, TSPO signal could mostly be observed within the reactive hypertrophic astrocytes and in

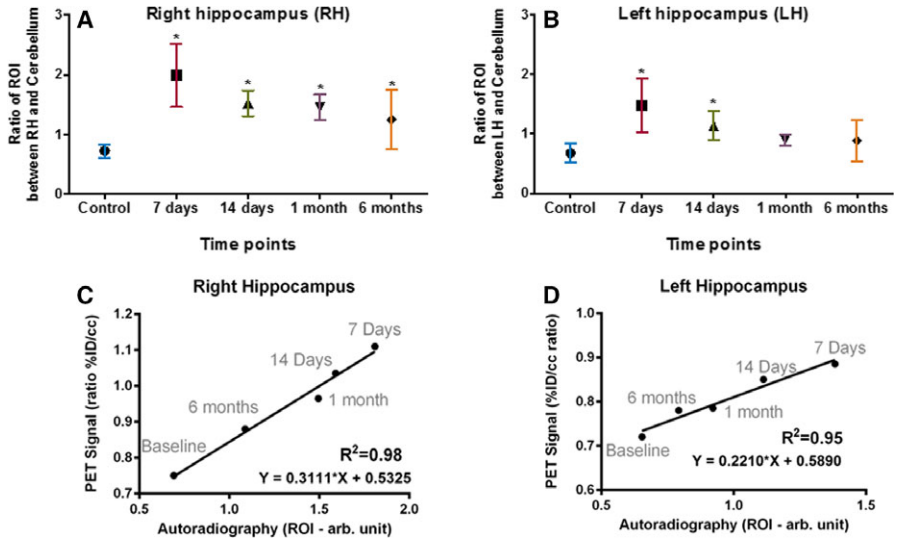

FIGURE 4 Autoradiography analysis shows an excellent correlation between translocator protein (TSPO) positron emission tomography (PET) signal and the specific TSPO signal observed ex vivo. A, B, Evolution of the in vitro ^{18}F-DPA-714 autoradiography signal in the right hippocampus and left hippocampus of kainic acid (KA) mice at different time points. The ratio of the percentage injected dose per cubic centimeter of tissue (%ID/cc) in the hippocampus to the cerebellum is presented (*P < .05). C, D, Correlation between PET signal (ratio between %ID in hippocampus and cerebellum) and autoradiography signal (region of interest [ROI] in arbitrary [arb.] units) at every time point (baseline, 7 days, 14 days, 1 month, and 6 months). The data points were fitted by a linear regression, showing a high coefficient of determination R^2 between the PET signal and the observed autoradiography signal (n = 6 mice for KA group for PET imaging and n = 3 for autoradiography for each time point)

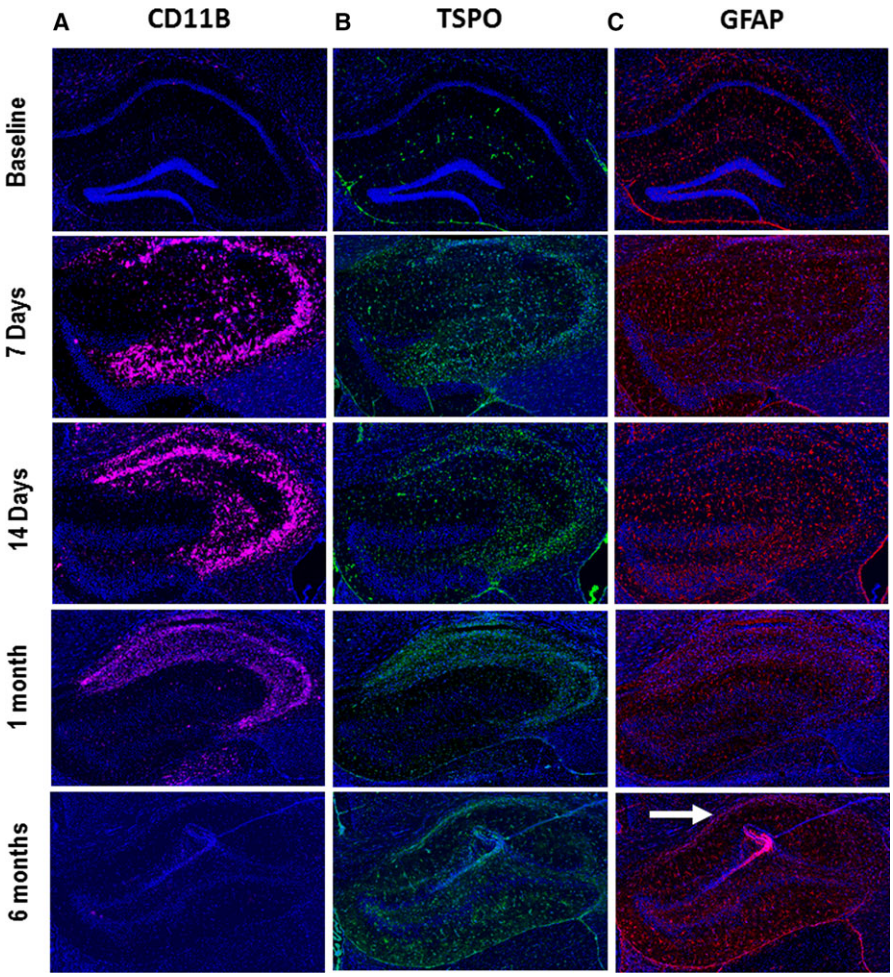

FIGURE 5 Glial cell evolution over time and translocator protein (TSPO) expression obtained using immunohistofluorescence in the right hippocampus of kainic acid mouse brain coronal slices. Triple staining was performed with A, CD11b for microglia (magenta); B, TSPO antibody for TSPO expression (green); and C, glial fibrillary acidic protein (GFAP) for astrocytes (red). Nuclei were counterstained with 4,6-diamidino-2-phenylindole (blue). The white arrow indicates the astrogliosis scar. Between 0 and 14 days, the TSPO signal is mainly due to reactive microglia, and after 14 days, there is a strong contribution to the TSPO signal coming from the reactive astrocytes

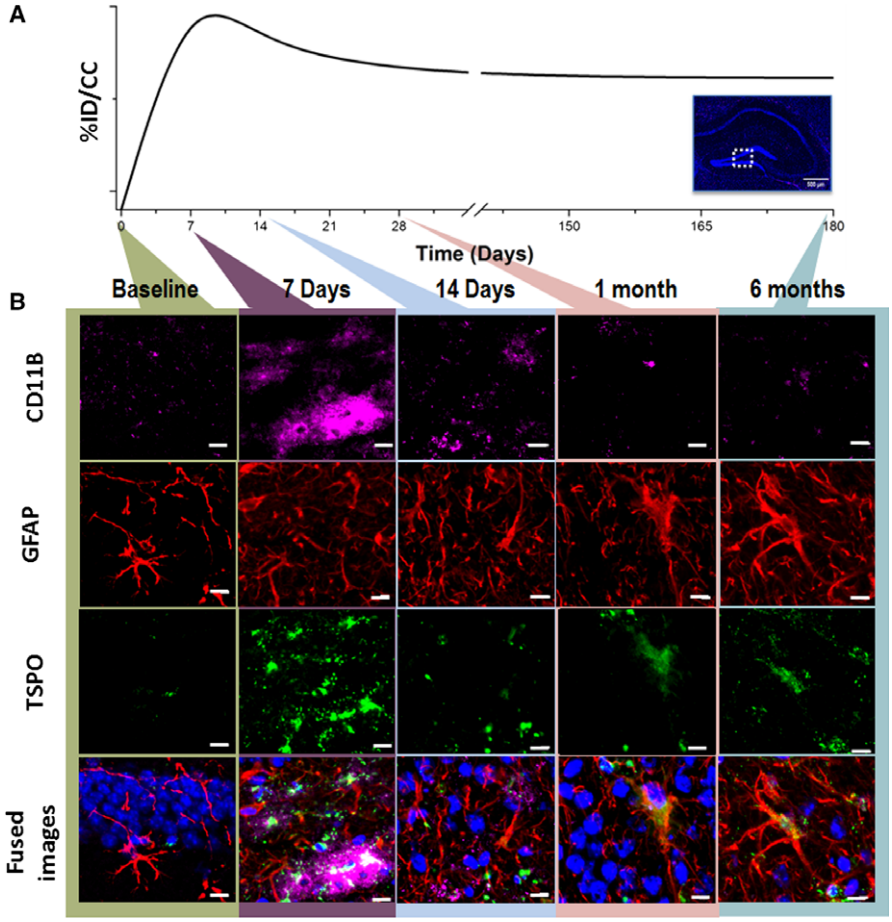

FIGURE 6 Correlation between the positron emission tomography translocator protein (TSPO) imaging, TSPO signaling, and glial cell activity. A, ^{18}F-DPA-714 uptake in the right hippocampus associated with the epilepsy stages. The data were fitted by a nonlinear model (least squares algorithm). B, Immunohistofluorescence staining images with CD11b (magenta), glial fibrillary acidic protein (GFAP; red), and TSPO (green) magnified at 20× with the fused images. Each stage of the epilepsy course could offer a therapeutic window. Scale bars = 50 μm. %ID/CC, percentage injected dose per cubic centimeter of tissue

the astrocytes forming scar (Figure 6). Some microglia/macrophages expressing TSPO were observed in the astrogliosis scar as well as some endothelial cells (Figure S7).

4 | DISCUSSION

This longitudinal study of 6 months has demonstrated the feasibility of using ^{18}F-DPA-714 PET to monitor neuroinflammation in vivo in a model of MTLE, even in small anatomical structures such as the mouse hippocampus. The TSPO signal seen within the HS persisted with time and came from activated microglia at 7 days and from the astrogliosis reaction later on, at 6 months after KA injection.

In line with recent studies using a systemic KA or pilocarpine rat model,[7,22] we observed peak uptake of ^{18}F-DPA-714 in the hippocampi 7 days after model induction. This phenomenon was also reported in different excitotoxic models such as the injection of quinolinic acid into the rat striatum[28] or KA into the rat thalamus.[29]

There is also a diffuse enhancement in extrahippocampal regions (Figure 2, shown in percentage injected dose) not seen on the autoradiography (Figure 3). This discrepancy could be either due to blood-brain barrier disturbance (as described in Breuher et al[30]) or due to more radiotracer availability in the blood. This emphasizes the need for the development of more sophisticated quantification methods.

Compared to the excitotoxic model in which the inflammatory signal is only localized in the neuron-depleted region, in the SE epilepsy model a high and diffuse signal could also be found in the limbic structure. These signals could be related to microglial activation modulating both the threshold and intensity of synaptic activity in local networks.[31] This modulation might prevent the severe and recurrent seizures present in SE and thus explain the silent period. In systemic models, it is difficult to distinguish the inflammatory signal from neuronal death caused by the systemic KA toxicity. In this mouse model, it was possible to observe neuroinflammation in the contralateral hippocampus, but no obvious cell loss was present. In line with Pernot et al,[20] we observed an activation of microglia in contralateral hippocampus. Interestingly, we observed that this activation was not found in pyramidal layers but was high in the strata. Different reasons can explain this phenomenon. One of the hypotheses is that this phenomenon could be related to microglial P2Y12 receptor-mediated process extension contacting neuronal dendrites to attenuate the seizures, playing a neuroprotective role.[32]

A first possible treatment window of interest is therefore in the early time points when the highest signal is coming from the microglia. In our study, we showed predominant microglial activation in the hilus and CA3 at early time points (7 days after KA injection). This could be explained by early neuronal death caused by the high affinity of KA receptors for KA in this region.[33] Microglia-mediated phagocytosis secreting different proinflammatory cytokines (tumor necrosis factor α, interleukin [IL]-1β, IL-6) in parallel has been shown to play a role in developing seizures.[34] Recently, more evidence also showed that anti-inflammatory treatments in this period such as IL-1β inhibition[35] or minocycline inhibiting microglial activation[36] can reduce chronic epileptic activity in KA mice.

A second possible treatment window is at later time points, when the highest signal is coming from the astrocytes. At later time points, Brackhan et al[22] showed that ^{11}C-PK11195 signal in the hippocampi declined toward baseline at 14-16 weeks after SE induced by pilocarpine. In the quinolinic acid rat model of excitotoxicity,[29] the TSPO signal and activated microglia also returned to baseline level in the lesion at 3 months after injection. In our study, the signal in the right hippocampus decreased but was still significantly higher compared to baseline in all KA mice (n = 8) even 6 months after induction, which is consistent with the ^{11}C-PBR28 PET study of epilepsy in patients with HS.[37]

For the first time, we demonstrated a high and persistent TSPO signal with PET imaging in the HS of a mouse model of epilepsy, which was shown to come from different components of a glial scar (severely reactive astrogliosis and accumulation of microglia/macrophages) and endothelial cells. Such glial scar formation has been found in different models of stroke or trauma that play essential roles in neural protection and repair. In these models, ablation of proliferating reactive astrocytes disrupting scar formation resulted in increased spread and persistence of inflammatory cells, and failure of repair of the blood-brain barrier inducing more neuronal loss.[38] However, astrogliosis could be either protective or harmful depending on the model disease, similarly to microglial activation. Reactive astrogliosis losing essential homeostatic capabilities has been demonstrated to contribute to the development of spontaneous seizures.[39] Rapamycin, an inhibitor of the mTOR pathway, could attenuate acute seizure-induced astrocyte injury in KA mice by restraining astrocyte proliferation and migration and production of inflammatory mediators, although there is no consensus on this and it requires further investigation.[40,41] Evaluation of this inhibitor when HS is established could open a new window for an effective treatment, which will be especially useful in epileptic patients, because the disease is usually diagnosed at the chronic stage.

TSPO-targeted PET allows for in vivo longitudinal monitoring of neuroinflammation associated with HS in a mouse model of MTLE. Combined with in vivo autoradiography and immunohistofluorescence, it revealed the different inflammatory components involved in the formation of hippocampal sclerosis in that model. The high TSPO persistent signal in the established HS could open a new treatment window in drug-resistant epilepsy.

DISCLOSURE

None of the authors has any conflict of interest to disclose. We confirm that we have read the Journal's position on issues involved in ethical publication and affirm that this report is consistent with those guidelines.

REFERENCES

1. Wiebe S, Jette N. Epilepsy surgery utilization: who, when, where, and why? Curr Opin Neurol. 2012;25:187–93.
2. Ravizza T, Gagliardi B, Noe F, et al. Innate and adaptive immunity during epileptogenesis and spontaneous seizures: evidence from experimental models and human temporal lobe epilepsy. Neurobiol Dis. 2008;29:142–60.
3. Gershen LD, Zanotti-Fregonara P, Dustin IH, et al. Neuroinflammation in temporal lobe epilepsy measured using positron emission tomographic imaging of translocator protein. JAMA Neurol. 2015;72:882–8.
4. Butler T, Li Y, Tsui W, et al. Transient and chronic seizure-induced inflammation in human focal epilepsy. Epilepsia. 2016;57:e191–4.
5. Bogdanović RM, Syvänen S, Michler C, et al. (R)-[11C]PK11195 brain uptake as a biomarker of inflammation and antiepileptic drug resistance: evaluation in a rat epilepsy model. Neuropharmacology. 2014;85:104–12.
6. Bertoglio D, Verhaeghe J, Santermans E, et al. Non-invasive PET imaging of brain inflammation at disease onset predicts spontaneous recurrent seizures and reflects comorbidities. Brain Behav Immun. 2017;61:69–79.
7. Amhaoul H, Hamaide J, Bertoglio D, et al. Brain inflammation in a chronic epilepsy model: evolving pattern of the translocator protein during epileptogenesis. Neurobiol Dis. 2015;82:526–39.
8. Vitaliti G, Pavone P, Mahmood F, et al. Targeting inflammation as a therapeutic strategy for drug-resistant epilepsies: an update of new immune-modulating approaches. Hum Vaccin Immunother. 2014;10:868–75.
9. Lavisse S, Guillermier M, Herard AS, et al. Reactive astrocytes overexpress TSPO and are detected by TSPO positron emission tomography imaging. J Neurosci. 2012;32:10809–18.
10. Chen MK, Guilarte TR. Translocator protein 18 kDa (TSPO): molecular sensor of brain injury and repair. Pharmacol Ther. 2008;118:1–17.
11. Mirzaei N, Tang SP, Ashworth S, et al. In vivo imaging of microglial activation by positron emission tomography with [(11)C]PBR28 in the 5XFAD model of Alzheimer's disease. Glia. 2016;64:993–1006.
12. Lartey FM, Ahn GO, Shen B, et al. PET imaging of stroke-induced neuroinflammation in mice using [18F]PBR06. Mol Imaging Biol. 2014;16:109–17.
13. Israel I, Ohsiek A, Al-Momani E, et al. Combined [(18)F]DPA-714 micro-positron emission tomography and autoradiography

imaging of microglia activation after closed head injury in mice. J Neuroinflammation. 2016;13:140.
14. Banati RB, Newcombe J, Gunn RN, et al. The peripheral benzodiazepine binding site in the brain in multiple sclerosis: quantitative in vivo imaging of microglia as a measure of disease activity. Brain. 2000;123(pt 11):2321–37.
15. Gargiulo S, Anzilotti S, Coda AR, et al. Imaging of brain TSPO expression in a mouse model of amyotrophic lateral sclerosis with (18)F-DPA-714 and micro-PET/CT. Eur J Nucl Med Mol Imaging. 2016;43:1348–59.
16. Winkeler A, Boisgard R, Awde AR, et al. The translocator protein ligand [(1)(8)F]DPA-714 images glioma and activated microglia in vivo. Eur J Nucl Med Mol Imaging. 2012;39:811–23.
17. Banati RB, Goerres GW, Myers R, et al. [11C](R)-PK11195 positron emission tomography imaging of activated microglia in vivo in Rasmussen's encephalitis. Neurology. 1999;53:2199–203.
18. Owen DR, Narayan N, Wells L, et al. Pro-inflammatory activation of primary microglia and macrophages increases 18 kDa translocator protein expression in rodents but not humans. J Cereb Blood Flow Metab. 2017;37:2679–90.
19. Bouilleret V, Ridoux V, Depaulis A, Marescaux C, Nehlig A, La Salle GL. Recurrent seizures and hippocampal sclerosis following intrahippocampal kainate injection in adult mice: electroencephalography, histopathology and synaptic reorganization similar to mesial temporal lobe epilepsy. Neuroscience. 1999;89:717–29.
20. Pernot F, Heinrich C, Barbier L, et al. Inflammatory changes during epileptogenesis and spontaneous seizures in a mouse model of mesiotemporal lobe epilepsy. Epilepsia. 2011;52:2315–25.
21. Riban V, Bouilleret V, Pham-Le BT, Fritschy JM, Marescaux C, Depaulis A. Evolution of hippocampal epileptic activity during the development of hippocampal sclerosis in a mouse model of temporal lobe epilepsy. Neuroscience. 2002;112:101–11.
22. Brackhan M, Bascunana P, Postema JM, et al. Serial quantitative TSPO-targeted PET reveals peak microglial activation up to 2 weeks after an epileptogenic brain insult. J Nucl Med. 2016;57:1302–8.
23. Brackhan M, Bascuñana P, Ross TL, et al. [18F]GE180 positron emission tomographic imaging indicates a potential double-hit insult in the intrahippocampal kainate mouse model of temporal lobe epilepsy. Epilepsia. 2018;59:617–26.
24. Damont A, Hinnen F, Kuhnast B, et al. Radiosynthesis of [18F]DPA-714, a selective radioligand for imaging the translocator protein (18 kDa) with PET. J Labelled Comp Radiopharm. 2008;51:286–92.
25. Ma Y, Hof PR, Grant SC, et al. A three-dimensional digital atlas database of the adult C57BL/6J mouse brain by magnetic resonance microscopy. Neuroscience. 2005;135:1203–15.
26. Paxinos G, Franklin KBJ. The mouse brain in stereotaxic coordinates. San Diego, CA: Academic Press; 2001.
27. Notter T, Coughlin JM, Gschwind T, et al. Translational evaluation of translocator protein as a marker of neuroinflammation in schizophrenia. Mol Psychiatry. 2018;23:323.
28. Arlicot N, Tronel C, Bodard S, et al. Translocator protein (18 kDa) mapping with [125I]-CLINDE in the quinolinic acid rat model of excitotoxicity: a longitudinal comparison with microglial activation, astrogliosis, and neuronal death. Mol Imaging. 2014;13:4–11.
29. Dusart I, Marty S, Peschanski M. Glial changes following an excitotoxic lesion in the CNS–II. Astrocytes. Neuroscience. 1991;45:541–9.
30. Breuher H, Meier M, Schneefeld S, et al. Multimodality imaging of blood-brain barrier impairment during epileptogenesis. J Cereb Blood Flow Metab. 2017;37:2049–61.
31. Xavier AL, Menezes JR, Goldman SA, Nedergaard M. Fine-tuning the central nervous system: microglial modelling of cells and synapses. Philos Trans R Soc Lond B Biol Sci. 2014;369:20130593.
32. Eyo UB, Murugan M, Wu LJ. Microglia-neuron communication in epilepsy. Glia. 2017;65:5–18.
33. Ben-Ari Y, Cossart R. Kainate, a double agent that generates seizures: two decades of progress. Trends Neurosci. 2000;23:580–7.
34. Vezzani A, French J, Bartfai T, Baram TZ. The role of inflammation in epilepsy. Nat Rev Neurol. 2011;7:31–40.
35. Maroso M, Balosso S, Ravizza T, et al. Interleukin-1beta biosynthesis inhibition reduces acute seizures and drug resistant chronic epileptic activity in mice. Neurotherapeutics. 2011;8:304–15.
36. Abraham J, Fox PD, Condello C, Bartolini A, Koh S. Minocycline attenuates microglia activation and blocks the long-term epileptogenic effects of early-life seizures. Neurobiol Dis. 2012;46:425–30.
37. Hirvonen J, Kreisl WC, Fujita M, et al. Increased in vivo expression of an inflammatory marker in temporal lobe epilepsy. J Nucl Med. 2012;53:234–40.
38. Sofroniew MV. Molecular dissection of reactive astrogliosis and glial scar formation. Trends Neurosci. 2009;32:638–47.
39. Robel S, Buckingham SC, Boni JL, et al. Reactive astrogliosis causes the development of spontaneous seizures. J Neurosci. 2015;35:3330–45.
40. Guo D, Zou J, Wong M. Rapamycin attenuates acute seizure-induced astrocyte injury in mice in vivo. Sci Rep. 2017;7:2867.
41. Shima A, Nitta N, Suzuki F, Laharie AM, Nozaki K, Depaulis A. Activation of mTOR signaling pathway is secondary to neuronal excitability in a mouse model of mesio-temporal lobe epilepsy. Eur J Neurosci. 2017;41:976–88.

SUPPORTING INFORMATION

Additional Supporting Information may be found online in the supporting information tab for this article.

How to cite this article: Nguyen D-L, Wimberley C, Truillet C, et al. Longitudinal positron emission tomography imaging of glial cell activation in a mouse model of mesial temporal lobe epilepsy: Toward identification of optimal treatment windows. *Epilepsia*. 2018;59:1234–1244. https://doi.org/10.1111/epi.14083